Oblique impact of rolling spheres: a generalization of billiard-ball collisions

A. Doménech Carbó and M.T. Doménech Carbó
I.B. Buñol, Instituto de Ciencia de los Materiales, Universidad de Valencia
Dr. Moliner, 50, Burjassot (Valencia) 46360. Spain

Recibido el 7 de enero de 1998; aceptado el 14 de agosto de 1998

A model for the inelastic collision of spheres rolling on a horizontal plane with arbitrary spins about horizontal and vertical axes is presented. This formulation includes an account of frictional forces acting between the spheres at impact. As a result, the scattering angles just after the collision and when the rolling motion is reestablished can be expressed as a function of the friction and restitution coefficients and the impact angle. A procedure is obtained to determine whether or not sliding takes place at the points of contact during impact. Theory is in agreement with experimental data for different materials, including billiard balls.

Keywords: Impact; friction; restitution

Se presenta un modelo para la descripción del choque entre esferas que ruedan sobre un plano horizontal con rotaciones arbitrarias en torno a ejes vertical y horizontales incorporando el efecto de las fuerzas de rozamiento durante el impacto. Como resultado, se obtienen los ángulos de desviación de las esferás inmediatamente después de la colisión y cuándo se alcanza nuevamente el régimen de rodadura pura en función de los coeficientes de rozamiento y restitución y del ángulo de impacto. Se discuten los casos en que existe y no existe deslizamiento entre los puntos de contacto de las esferas durante el choque. Los datos experimentales para esferas de distintos materiales, incluyendo bolas de billar, se hallan en buen acuerdo con la teoría.

Descriptores: Choque; rozamiento; restitución

PACS: 05.50.Kw

1. Introduction

Collisions between rolling spheres and, in particular, billiard-ball collisions are frequently mentioned in texts to illustrate the application of classical laws of conservation. However, the detailed analysis of all the factors influencing the observed postcollision trajectories in rolling ball collisions is rarely accounted for. First of all, the impact event can be considered as elastic or inelastic, whether tangential forces are taken into account or not. Secondly, the paths of the balls after the impact are curved by effect of the friction between the balls and the supporting surface.

Figure 1 illustrates the collision between a rolling cue ball and a stationary object ball. Immediately after the impact, the balls move in directions that form postcollision angles, α_j (or δ_j; $j = 1, 2$) with the initial direction of the cue ball. The motion of the balls is then a combination of rolling and sliding so that this friction with the supporting surface causes each sphere to describe a curved path until it rolls without slipping in a straight line. Then, the balls move in directions that define postransition angles β_j (or ϑ_j).

A limited number of approaches have been published: Bayes and Scott [1] studied billiard-ball collisions on a low-friction surface to prevent curved trajectories after impact. These authors assumed inelasticity and absence of tangential forces during the impact event. In 1968, Armstrong discussed [2] the head-on impact of rolling spheres taking into account the friction between them, but assuming the impact to be perfectly elastic. In 1988, Wallace and Schroeder [3] formulated the oblique impact of a cue ball in pure rolling motion against a stationary object ball assuming elasticity and absence of tangential forces at impact. On the basis of the Wallace and Schroeder model, Onoda [4] developed some practical rules for billiard games. More recently, Beltrán [5, 6] has presented a geometrical method for teaching collisions on the basis of the elastic frictionless model.

The scope of these models is limited by the prescription of initial pure rolling motion and the assumption of negligeable frictional effects at impact. As described qualitatively by Walker [7], the frictionless model is unable to explain the observed postcollision paths in billiard games when: *(a)* a cue ball hits an object ball that is already touching another object ball (the two object balls are said to be frozen); *(b)* a cue ball with left or right pivoting angular velocity (or "English" spin) rebounds from the rail. Thus, Jiménez [8, 9] discussed friction effects on billiard-ball collisions while Salazar and Sánchez-Lavega [10] and De la Torre [11] have studied the conditions that determine the motion of a billiard ball being tapped by a rod emphasizing the effect of friction on the kinematic state of the ball after the hit.

To study these impact events it is convenient to describe the motion of a billiard ball as being two simultaneous spins, one about a horizontal axis (topspin or backspin; "follow" or "drawn", respectively, in billiard terminology), and another about a vertical axis (left and right "English" in billiard terminology [12, 13]).

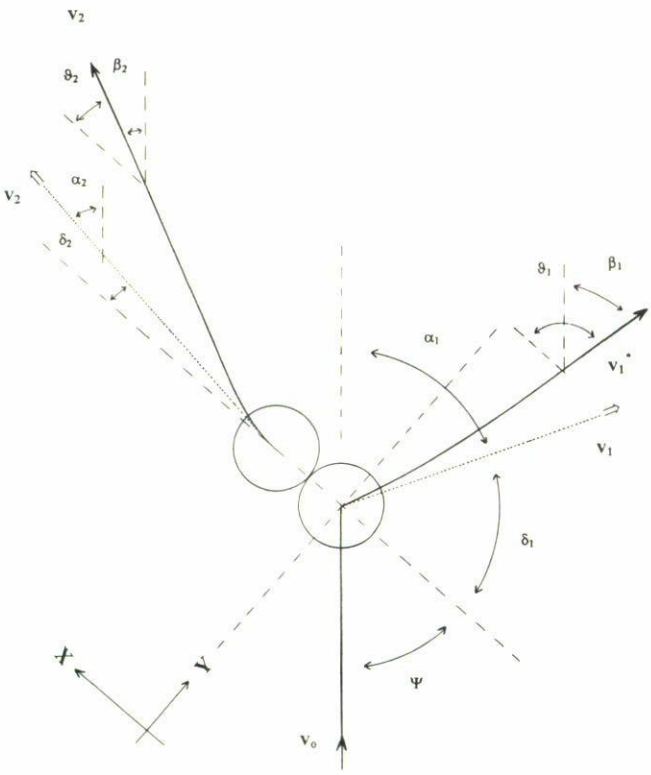

FIGURE 1. Schematic diagram of a cue ball and an object ball collision including postcollision and postransition angles. Solid lines represent the real curved paths of the balls and dotted lines correspond to the direction of the balls immediately after the impact.

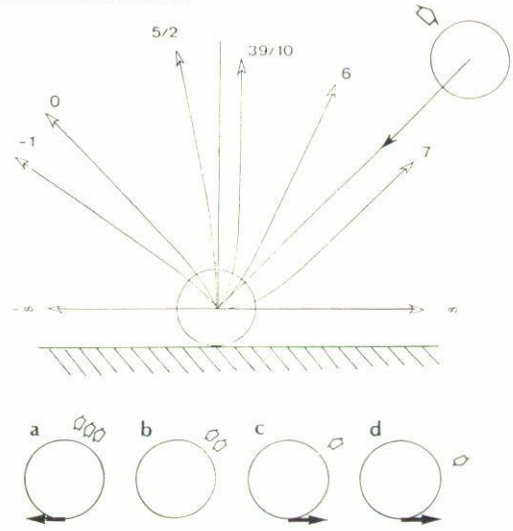

FIGURE 2. Rebound paths for the collisions of a rolling ball against a rigid vertical surface for various initial pivoting angular velocities expressed by the values of the quotient $R\Omega_0/v_0 \sin\psi$. It is assumed that the impact is perfectly elastic and occurs without sliding at the point of contact.

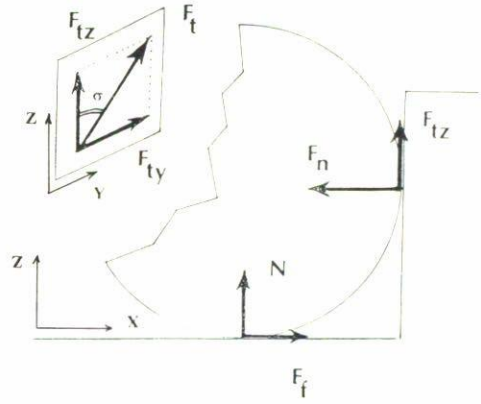

FIGURE 3. Impact of a rolling sphere against a rigid vertical surface band and scheme for frictional forces developed during the duration of the impact.

As schematized in Fig. 2, for the impact of a rolling ball against a rigid cushion, tangential forces acting throughout the impact must be necessarily included to explain the observed differences in the rebound angle, and, in particular, to explain the fact that for sufficiently large backspin pivotment, the ball may be projected backwards after the collision.

The purpose of the current paper is to offer a solution to the collision problem in the most general situation in which the cue ball has arbitrary values of inital rotation and pivotment (English) spins, *i)* by considering simultaneously the inelasticity of the impact and effects associated with frictional forces acting during the impact event; *ii)* including an account of subsequent friction with the supporting surface.

The approach presented here is an extension of prior studies on the frontal impact of rolling spheres [14] and oblique pendulum [15] and disc [16] collisions that are based on the general algorithms of Brach [17] and Kane and Levinson [18]. These authors emphasize the existence of two possible regimes of impact derived from the account of tangential forces: with and without sliding between the contacting surfaces. Collisions with sliding are recently described in detail by Keller [19]. Description of billiard ball collisions is complicated by the fact that impulsive forces act, during the impact event, not only between the balls but also between the balls and the supporting surface. Accordingly, we assume explicitly with regard to the impact event that [17–19]:

a) As represented in Fig. 3 for the impact with a rigid barrier, the impulsive forces acting throughout the impact can be described as a normal retarding force (F_n) plus a tangential force (F_t). For convenience, the tangential force will be divided into two components, F_{t_y}, F_{t_z}.

b) Tangential forces at impact will be treated as frictional forces inserting the coefficients of static (μ_0) and kinetic (μ) friction. Then, when sliding exists at the contacting points during the collision, the friction force is μ times the normal retarding force: $F_t = \mu F_n$.

c) The normal impulsive force (N) in Fig. 3 ensures that the ball moves along the horizontal supporting surface.

d) Eventually, additional impulsive frictional forces F_f acting between the spheres and the supporting horizontal surface appear. As can be deduced from Fig. 3,

under sliding conditions, F_f equals $\mu' N$, μ' being the coefficient of friction between the spheres and the supporting surface and N the corresponding normal impulsive force. The magnitude of F_f will be in general largely less than F_n (For a head-on impact with a vertical surface, $N = \mu F_n$ and $F_f = \mu' \mu F_n$). To simplify, effects associated with impulsive friction with the supporting surface will be neglected.

e) The impact is regarded as inelastic, inelasticity being expressed in terms of the coefficient of restitution, e. Coefficients of restitution and friction will be considered as constants dependent on the materials of which the balls are made, but not on their radii or velocities.

f) In general, relative tangential motion always exists during the time interval of contact between colliding bodies. However, under certain conditions, friction can be high enough to make this motion cease during the duration of impact and so no sliding takes place at collision.

g) In both cases, it is assumed that the direction of the impulsive tangential force is that of the relative tangential velocity of the contacting points of the spheres at the beginning of impact.

For postransition angles we depart from the formulation developed by Hopkins and Patterson [20], for the path of a bowling ball, further applied by Wallace and Schroeder [3], and Salazar and Sánchez-Lavega [10], for the study of the motion of a ball after being struck by a tapering rod. It should be noted that the functional form of the frictional force determines the precise nature of the curved path; however, the final direction of motion is completely independent of the nature of frictional force.

As a result of this analysis, one obtain a set of velocity-independent equations that relates the postcollision and postransition angles with the coefficients of restitution and friction and the ratio of masses. The model presented here contains the foregoing formulations as asymptotical cases [1–9].

In the experimental section these relationships are tested using a single experiment suitable for undergraduate laboratories.

2. Two-sphere collisions with sliding

2.1. Postcollision angles

Let us consider the oblique collision of a cue ball with an identical object ball which is initially placed at rest on a rough horizontal plane. Here, we consider the general case in which the cue sphere rolls and slips with arbitrary center-of-mass velocity, v_0, and arbitrary angular velocity, ω_0, perpendicular to the linear velocity. In addition, an arbitrary pivoting rotation around a vertical axis ("English") with angular velocity Ω_0 is superimposed on the rolling and slipping motion of the cue ball.

As schematized in Fig. 1, a normal-tangential coordinate system is chosen such that the line through the ball centers is the normal (x) axis. The tangential axis (y) is perpendicular to the normal axis and lies in the plane of velocities. Conservation of momentum along the tangential and normal axes gives, respectively,

$$m_1 v_0 \sin\psi = m_1 v_1 \sin\delta_1 + m_2 v_2 \sin\delta_2, \tag{1}$$

$$m_1 v_0 \cos\psi = m_1 v_1 \cos\delta_1 + m_2 v_2 \cos\delta_2, \tag{2}$$

where $v_j (j = 1, 2)$ represents the horizontal velocites immediately after collision, and m_i the masses of the spheres. ψ represents the impact angle and δ_j, denotes the postcollision angles defined with respect to the line of centers, as shown in Fig. 1.

The inelasticity of impact is expressed in terms of the coefficient of restitution, e, defined as the negative ratio of the relative velocities before and after the impact [11]. Thus,

$$v_2 \cos\delta_2 - v_1 \cos\delta_1 = e v_0 \cos\psi. \tag{3}$$

Combining these above equations, and introducing the ratio of the masses, $M = (m_1/m_2)$, gives

$$\tan\delta_1 = \left(\frac{1+M}{M-e}\right)\tan\psi - \left(\frac{1+e}{M-e}\right)\tan\delta_2. \tag{4}$$

The effect of frictional forces at impact can be rationalized by considering the simple case of the rebound of a rolling ball with a vertical rough surface, depicted in Figs. 2 and 3. Consider a ball with radius R that is thrown with an initial forward spin at the point of contact with rotational velocity $R\,\Omega_0$ opposite to the horizontal translational velocity component $(v_0 \sin\psi)$ of the ball. If the spin rate is high enough $(R\,\Omega_0 > v_0 \sin\psi)$ the horizontal component of friction force will act in the forward direction. In this case, there will be a gain in horizontal velocity and a decrease in pivoting angular velocity (Fig. 2a). When the spin rate equals the horizontal translational velocity component $(R\,\Omega_0 = v_0 \sin\psi)$ of the ball, there is no horizontal friction force acting on the sphere (Fig. 2b). When $(R\,\Omega_0 < v_0 \sin\psi)$, the friction force acts in the backward direction (Fig. 2c), and, finally, if the ball is projected with a backspin then the friction force opposes both the translational and rotational motions. Consequently, a ball projected forward with backspin will lose considerable speed on the collision and may even bounce backwards (Fig. 2d).

Similarly, a vertical frictional force arises at the point of contact which alters the horizontal angular velocity of the sphere. For the two-sphere collision schematized in Fig. 1, action of frictional forces must cause not only a change in the horizontal and vertical angular velocitites, but also a deviation of the object ball from the line joining the centers of the spheres at impact.

Assuming that the direction of the resulting tangential force is that of the relative tangential velocity of the contacting points of the spheres at the beginning of impact, the angle

of inclination of the frictional force (see Fig. 3), σ, will be derived from the quotient between the horizontal and vertical components of friction force:

$$\tan\sigma = \frac{v_0 \sin\psi + R\,\Omega_0}{R\,\omega_0 \cos\psi}. \tag{5}$$

If sliding occurs between the points of contact, and the slip direction remains constant throughout the collision, the frictional impulse is the coefficient of friction times the magnitude of the normal impulse, *i.e.*,

$$m_1(v_0 \sin\psi - v_1 \sin\delta_1) = \mu m_1 \sin\sigma(v_0 \cos\psi - v_1 \cos\delta_1), \tag{6}$$

$$m_2 v_2 \sin\delta_2 = \mu m_2 v_2 \sin\sigma \cos\delta_2. \tag{7}$$

Equation (7) reduces to

$$\tan\delta_2 = \mu \sin\sigma. \tag{8}$$

And, then, Eq. (4) becomes,

$$\tan\delta_1 = \left(\frac{1+M}{M-e}\right)\tan\psi - \mu\left(\frac{1+e}{M-e}\right)\sin\sigma. \tag{9}$$

These equations express the postcollision angles as a function of the impact angle which can be experimentally tested. The model of Bayes and Scott [1] corresponds to $R\,\omega_0/v_0 = 1$, $\Omega_0 = 0$, in the limiting case in which $\mu = 0$. For the ideal elastic ($e = 1$) frictionless ($\mu = 0$) case, Eq. (9) leads to $\alpha_2 = \psi$ and, $\alpha_1 + \alpha_2 = 90°$; *i.e.*, reduces to the well known 90° angle rule.

Postcollision velocities can be expressed in terms of the initial velocity and the impact angle as:

$$v_{1x} = v_0\left(\frac{M-e}{1+M}\right)\cos\psi, \tag{10}$$

$$v_{1y} = v_0\left[\sin\psi - \mu\left(\frac{1+e}{1+M}\right)\sin\sigma\cos\psi\right], \tag{11}$$

$$v_{2x} = v_0 M\left(\frac{1+e}{1+M}\right)\cos\psi, \tag{12}$$

$$v_{2y} = v_0\mu M\left(\frac{1+e}{1+M}\right)\sin\sigma\cos\psi. \tag{13}$$

Changes in topspin or backspin are caused by vertical component of tangential forces whereas changes in the rotation of pivotment (right or left "English") are due to their horizontal components. The angular velocities for the spinning rotation of the balls just after impact can be derived from the law of angular momentum, by considering the momentums of the frictional forces acting between the spheres at impact. In differential form: $I_j d\Omega_j = \mu R \sin\sigma m_j dv_{jx}$, $I_j d\omega_{jy} = \mu R \cos\sigma m_j dv_{jx}$, $I_j d\omega_{jx} = 0$. As a result

$$\mathrm{R}\omega_{1y} = \mathrm{R}\omega_0 \cos\psi - \frac{5}{2}v_0\mu M\left(\frac{1+e}{1+M}\right)\cos\sigma\cos\psi, \tag{14}$$

$$\mathrm{R}\omega_{1x} = \mathrm{R}\omega_0 \sin\psi, \tag{15}$$

$$\mathrm{R}\omega_{2y} = \frac{5}{2}v_0\mu M\left(\frac{1+e}{1+M}\right)\cos\sigma\cos\psi, \tag{16}$$

$$\mathrm{R}\omega_{2x} = 0, \tag{17}$$

$$\mathrm{R}\Omega_1 = \mathrm{R}\Omega_0 - \frac{5}{2}v_0\mu\left(\frac{1+e}{1+M}\right)\sin\sigma\cos\psi, \tag{18}$$

$$\mathrm{R}\Omega_2 = -\frac{5}{2}v_0\mu M\left(\frac{1+e}{1+M}\right)\sin\sigma\cos\psi. \tag{19}$$

2.2. Postransition angles

As previously mentioned, vertical frictional forces must produce a change in the angular velocity of the spheres in such a way that their motion immediately after the impact will be a combination of rolling and sliding. Thus, friction with the supporting surface creates a torque about the center of gravity of the ball so that both the translational and rotational motions of the balls change until the rolling motion is established. The components of the linear velocity when the pure rolling motion occurs, v^*_{jx}, v^*_{jy}, verify $v^*_{jy} = \mathrm{R}\omega_{jx}$, and $v^*_{jx} = \mathrm{R}\omega_{jy}$.

The law of angular momentum corresponding to the torque of the friction force with the supporting surface, can be applied independently to motion in both the x and y directions. Then, integrating the equations $I_j\,d\omega_{jx} = -\mathrm{R}m_j\,dv_{jy}$ and $I_j\,d\omega_{jy} = -\mathrm{R}m_j\,dv_{jx}$, yields, for the components of the velocities when pure rolling motion occurs, $v^*_j (j = 1, 2)$:

$$v^*_{jx} = \frac{2}{7}\mathrm{R}\omega_{jy} + \frac{5}{7}v_{jx}, \tag{20}$$

$$v^*_{jy} = \frac{2}{7}\mathrm{R}\omega_{jx} + \frac{5}{7}v_{jy}. \tag{21}$$

Combining the equations for the linear and angular velocities after impact [Eqs. (10)–(19)], the velocity-independent expressions of the postransition angles, β_j (or ϑ_j), can be derived from $\tan\vartheta_j = v^*_{jy}/v^*_{jx}$:

$$\tan\vartheta_1 = \tan(\beta_1 + \psi) = \frac{(1+M)\left(k+\frac{5}{2}\right)\tan\psi - \frac{5}{2}\mu(1+e)\sin\sigma}{(1+M)\,k + \frac{5}{2}(M-e) - \frac{5}{2}\mu(1+e)\cos\sigma}, \tag{22}$$

$$\tan\vartheta_2 = \tan(\psi - \beta_2) = \frac{\mu\sin\sigma}{1-\mu\cos\sigma} \tag{23}$$

where $k = R\,\omega_0/v_0$. These equations reduce again to that of the frictionless model [3] by inserting $M = 1$, $e = 1$, $\mu = 0$, $\Omega_0 = 0$, and $k = 1$. In this case, Eq. (23) yields $\beta_2 = \alpha_2 = \psi$; *i.e.*, the ball after being initially at rest then moves along the line of centers at impact.

3. Two-sphere collisions without sliding

3.1. Postcollision angles

For high values of the frictional impulse, however, relative tangential motion should cease during the time interval of impact. If sliding ceases during contact, the horizontal and vertical components of the tangential velocities of the contact points of both spheres, must be equal immediately after the collision [17, 18]. For the horizontal velocities this requires:

$$v_1 \sin\delta_1 + R\Omega_1 = v_2 \sin\delta_2 + R\Omega_2. \tag{24}$$

Combining Eqs. (4), (6), (7), and (24), we arrive at the following condition of no slipping,

$$R\Omega_0 - \frac{5}{2}v_0 \sin\psi = \frac{7}{2}v_2 \sin\delta_2 - \frac{7}{2}v_1 \sin\delta_1. \tag{25}$$

From Eqs. (1), (2), (3), (5), and (25), we obtain,

$$\tan\delta_1 = \frac{1+M}{M-e}\tan\psi - \frac{\frac{2}{7}k}{M-e}\tan\sigma. \tag{26}$$

$$\tan\delta_2 = \frac{\frac{2}{7}k}{1+e}\tan\sigma. \tag{27}$$

Equations (8), (9), (26), and (27), are valid for arbitrary values of the masses and velocities of the balls and for arbitrary spinning rotation. The postcollision angles α_j can easily be obtained from this set of equations by inserting the relationships $\delta_1 = \pi - (\alpha_1 + \psi)$, and $\delta_2 = \psi - \alpha_2$.

This situation is quite similar to the familiar problem of a block slipping along a slanted plane. In general, for small impact angles collisions without sliding occur and then the tangential impulsive forces are $(2k/7)(1+e)\cos\sigma$ times the normal forces. The beginning of slipping takes place at a limiting impact angle, $\psi_{\rm L}$, where tangential forces reach their maximum value, $F_t = \mu_0 F_n$. For $\psi > \psi_{\rm L}$, tangential impulsive forces remain constant and equal to μ times the normal forces.

The critical impact angle, σ_L, where no sliding occurs at impact can be obtained inserting the static cofficient of friction, μ_0, into Eq. (8) and comparing it with Eq. (27):

$$\cos\sigma_{\rm L} = \frac{2k}{7\mu_0(1+e)}. \tag{28}$$

This equation reduces to $\tan\psi_{\rm L} = 2/7\mu_0(1+e)$ when the cue ball is initially in pure rolling motion without pivoting spin. Interestingly, in all cases $\psi_{\rm L}$ is independent of the masses of the balls.

3.2. Postransition angles

As in the case of collisions with sliding, linear and angular velocities just after the impact can be expressed as a function of impact angle and the initial velocity of the cue ball. For v_{1x}, v_{2x}, $R\omega_{1x}$, and $R\omega_{2x}$, Eqs. (10), (12), (15), and (17) hold, whereas for the other velocities the following equations apply:

$$v_{1y} = v_0\left[\sin\psi - \frac{2}{7}\left(\frac{k}{1+M}\right)\tan\sigma\cos\psi\right], \tag{29}$$

$$v_{2y} = \frac{2}{7}v_0 M\left(\frac{k}{1+M}\right)\tan\sigma\cos\psi, \tag{30}$$

$$R\omega_{1y} = R\omega_0\cos\psi - \frac{5}{7}v_0\left(\frac{k}{1+M}\right)\cos\psi, \tag{31}$$

$$R\omega_{2y} = \frac{5}{7}v_0 M\left(\frac{k}{1+M}\right)\cos\psi, \tag{32}$$

$$R\Omega_1 = R\Omega_0 - \frac{2}{7}v_0\left(\frac{k}{1+M}\right)\tan\sigma\cos\psi, \tag{33}$$

$$R\Omega_2 = -\frac{5}{7}v_0 M\left(\frac{k}{1+M}\right)\tan\sigma\cos\psi. \tag{34}$$

Inserting the equations for the linear and angular velocities after impact into Eqs. (20) and (21), a second set of velocity-independent expressions of the postransition angles, β_1, β_2, can be derived:

$$\tan(\beta_1+\psi) = \frac{[(1+M)\left[1+\frac{2}{5}k\right]\tan\psi - \frac{2}{7}\tan\sigma}{M - e + \frac{2}{5}(1+M)k - \frac{2}{7}k}, \tag{35}$$

$$\tan(\psi-\beta_2) = \frac{k\tan\sigma}{\frac{7}{2}(1+e)-k}. \tag{36}$$

4. Impact with a rigid barrier

4.1. Postcollision angles

The case in which a rolling ball strikes a rigid vertical surface is schematized in Fig. 4. As before, we assume that the direction of tangential force is that of the relative tangential velocity of the contacting points of the spheres at the beginning of impact. So, for collisions with sliding it is possible write

$$v\cos\delta = ev_0\cos\psi, \tag{37}$$

$$v_0\sin\psi - v\sin\delta = \mu v_0(1+e)\cos\psi\sin\sigma, \tag{38}$$

where v is the horizontal velocity of the mass center of the ball after impact.

Combining Eqs. (37) and (38) gives

$$\tan\delta = \frac{1}{e}\tan\psi - \frac{\mu}{e}(1+e)\sin\sigma. \tag{39}$$

When friction is sufficient to produce collision without sliding, the following condition holds: $R\Omega\cos\psi = v\sin\delta$. Then,

$$\tan\delta = \frac{1}{e}\tan\psi - \frac{2}{7e}k\tan\sigma. \tag{40}$$

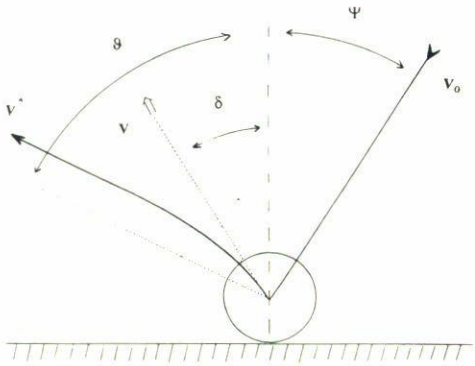

FIGURE 4. Postcollision and postransition angles in the rebound of a rolling ball against a rigid vertical surface.

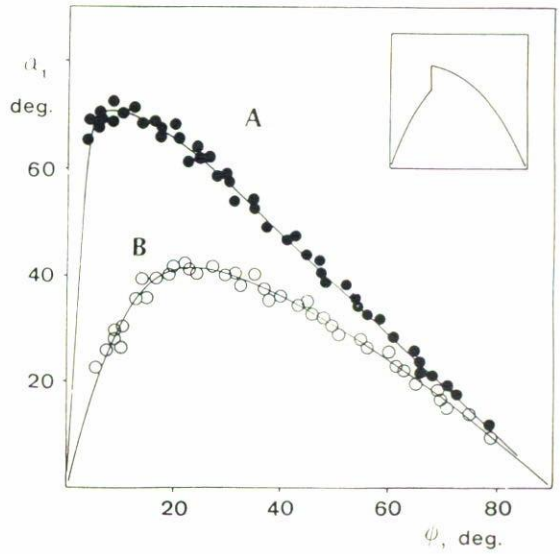

FIGURE 5. Plots of the postcollision cue ball angle (α_1) *versus* the impact angle (ψ) for collisions between: A: billiard spheres; B: brass spheres. Lines correspond to theoretical values from Eqs. (9) and (26) inserting $e = 0.97, \mu = 0.07$ and $e = 0.65, \mu = 0.15$, for billiard balls and brass spheres, respectively. Inset represents the theoretical representations.

4.2. Postransition angles

A similar treatment to that previously developed [Eqs. (20)–(23)] leads, for linear velocities at the instant at which pure rolling motion is reestablished, to $v_x^* = (2/7)R\omega_y + (5/7)v\sin\delta$, and $v_y^* = (5/7)v\cos\delta - (2/7)R\omega_x$. From the above set of equations, the postransition angles for collisions with sliding are obtained:

$$\tan\vartheta = \frac{\frac{7}{5}\tan\psi - \mu(1+e)\sin\sigma}{e - \frac{2}{5} + \mu(1+e)\cos\sigma}, \tag{41}$$

and, for collisions without sliding,

$$\tan\vartheta = \frac{\frac{5}{2} + k\tan\psi - \frac{5}{7}k\tan\sigma}{\frac{5}{2}e - \frac{2}{7}k}, \tag{42}$$

5. Experimental

Experiments of collisions of a cue ball, *i)* with a stationary object ball, and, *ii)* with a vertical surface were carried out on a laboratory bench and, eventually, a regulation billiard table. The velocity of the cue ball was adjusted to 0.80 ± 0.10 m/s using a slanted track. In all cases, the distance from the edge of the track to the object ball was great enough to ensure pure rolling motion of the cue ball before impact. In addition to regulation billiard balls, brass and steel spheres of 2.50 cm diameter were used.

The angles of impact, postcollision and postransition were determined from the photographs obtained with a camera placed in cenital position. Conventional light sources led to satisfactory angle measurements. Alternatively, the trajectories of the balls were recorded with the help of a carbon paper with comparable results. Accuracy in the angle measurements is estimated as $\pm 1°$.

To check our predictions concerning the influence of the initial spin conditions, subsequent series of experiments were performed. These experiments measured the angles of impact and rebound of a ball striking a vertical wooden surface *iii)* after being struck by auxiliary cue ball, and, *iv)* after a prior impact with an auxiliary vertical surface. As a result of the first impact, the cue ball acquires an English spin conditioning postcollision and postransition angles in the second impact. Different series of data were then obtained by varying the angle of impact with the auxiliary ball or with the auxiliary plane, resulting in selected values of angular velocity or pivotment.

6. Results and discussion

6.1. Rolling ball collisions

Qualitatively, the current model makes some specific predictions in contrast with the elastic frictionless model:

a) The 90° angle rule does not apply, for both postransition angles and postcollision angles.

b) The direction of motion of ball 2 after impact diverges from the line joining the centers at collision.

c) After collision, not only the trajectory of ball 1, but also that of ball 2 is curved.

Experimental data confirms all these predictions and shows a satisfactory agreement with quantitative predictions in our experimental conditions. The dependence of the postcollision and postransition angles upon the impact angle for steel and brass spheres is shown in Figs. 5, 6 and 7. In all these figures, points denote experimentally determined values while the solid lines indicate the anticipated theoretical

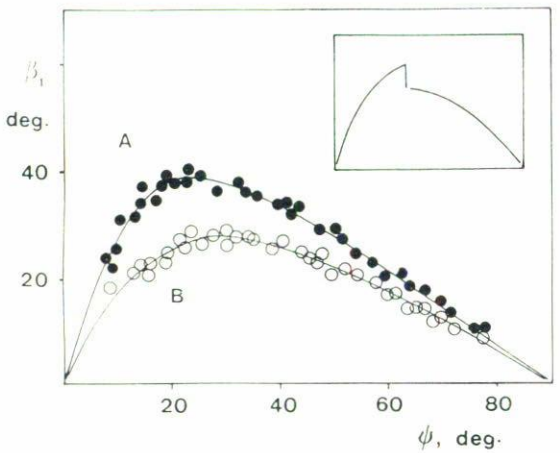

FIGURE 6. Plots of the postransition angle (β_1) *versus* the impact angle (ψ) for collisions between: A: steel spheres; B: brass spheres. Lines correspond to theoretical values from Eqs. (22) and (35) inserting $e = 0.95, \mu = 0.15$ and $e = 0.65, \mu = 0.15$, for billiard balls and brass spheres, respectively. Inset represents the theoretical representations.

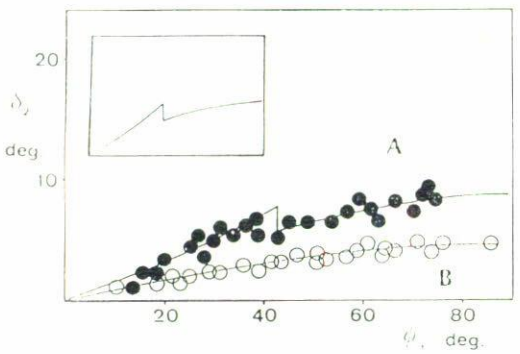

FIGURE 7. Plots of δ_2 *vs.* ψ for the collisions between A: two brass spheres; B: two regulation billiard balls. Points: experimental data. Solid lines represent the theoretical values from Eqs. (8) and (27) inserting A: $e = 0.65$ and $\mu = 0.15$; B: $e = 0.97$ and $\mu = 0.07$.

dependence. Insets in these figures show the theoretical dependence for each one of the corresponding representations. The "jumps" that separate these portions from each other occur because the static and kinetic friction coefficients differ from each other. When the calculations are performed with equal values of the two friction coefficients, these discontinuities disappear, but discontinuities in slope remain at points of transition from collisions involving sliding at the instant of separation to those not involving sliding at this instant.

For all postcollision and postransition angles, an excellent agreement was found between theory and experiment inserting into theoretical equations the values $e = 0.95, \mu = 0.15$ for steel spheres, and, $e = 0.65, \mu = 0.15$ for brass spheres. For collisions between two billiard balls, the values $e = 0.97$ and $\mu = 0.07$ provided the best fit of the experimental data with theory. These parameter values correspond to collisions with slipping for all impact angles. This fact is directly derived from the slow friction (compare curves A and B in Fig. 7) coefficient between billiard balls. The e values are in agreement with the values reported by Bayes and Scott [1].

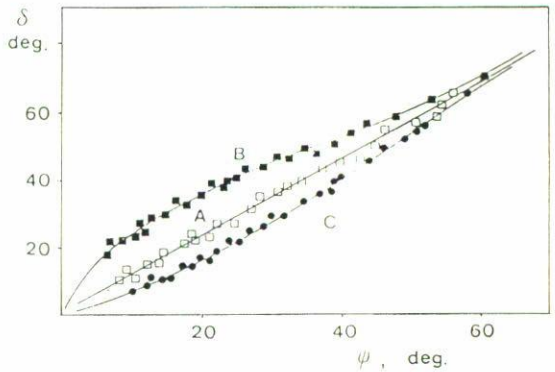

FIGURE 8. Plots of the rebound angle, δ, *versus* the impact angle for collisions of a steel ball with a vertical wooden surface. Initial pivotment spin imparted by a prior impact. Experimental data (squares) and theoretical values from Eqs. (39) and (40) inserting $e = 0.60, \mu = 0.18$. A: forward spin ($R\Omega_0/v_0 = -0.30$); B: no initial spin ($R\Omega_0 = 0$); C: backspin ($R\Omega_0/v_0 = 0.30$).

It should be noted that, for these parameter values, equations of the α_1 and β_1 angles for collisions with sliding yield angle values almost identical than those calculated from the no sliding equations and no direct estimates of the static coefficient of friction values were obtained. Nevertheless, experimental data limited them to values 20% above the kinetic coefficient in all cases. This can be seen in Fig. 7, which shows experimental data for collisions between brass spheres, and theoretical plots of δ_2 *versus* ψ inserting $e = 0.65, \mu = 0.15$ and $\mu_0 = 0.20$ into Eqs. (8), (27), and (28).

Confirming the consistency of the model, experimental postransition angles for collisions between steel and brass spheres agree well with the theoretically anticipated data when the above values of the coefficients of restitution and friction are inserted.

Theoretical equations for collisions with initial "English" spin were confirmed by experiments in which a ball, initially at rest, collides against a vertical surface after being struck by an identical cue ball or after impact with an auxiliary vertical surface. Comparison of theory with experiment requires a suitable estimate of the angle σ or the ratio $R\Omega_0/v_0$, which represents the initial forward or backward spin acquired by the sphere. The ratio $R\Omega_0/v_0$ can be calculated from Eqs. (19) and (34), providing the value of the fixed angle of impact and other parameters involved are known (e for collisions without sliding, and μ and e for collisions with sliding). Figure 8 represents the variation of the rebound angle with the impact angle for the collisions of a steel sphere against a wooden surface, the ball being impulsed by an auxiliary steel sphere colliding with an impact angle of $\psi = 45°$. The experimental results for negative (A), zero (B), and positive (C) spin agree well with the predictions of Eqs. (40) and (45) substituting $e = 0.60, \mu = 0.18$, and the calculated values of $R\Omega_0/v_0$ equal to $-0.30, 0$ and $+0.30$, respectively.

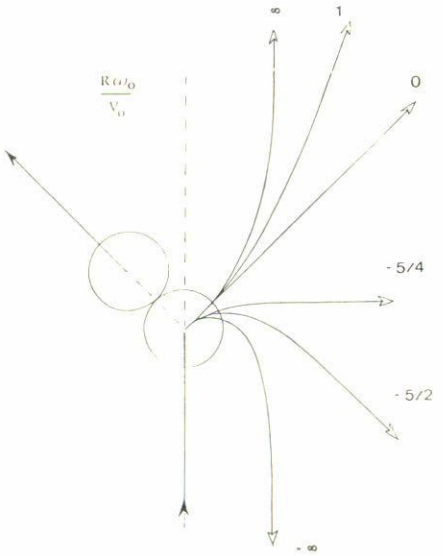

FIGURE 9. Schematic representations of postcollision paths for the elastic ($e = 1$) frictionless ($\mu = 0$) impact (impact angle 45°) of a cue ball against a stationary ball for selected k values.

7. Final considerations

It should be noted that the scope of the current model is limited by the confidence level of simplifying assumptions concerning the constancy of the coefficients of restitution and friction. Strictly, coefficients of restitution [21, 22] and friction [23, 24] depend on several factors, the relative velocity of contacting bodies in particular. In our experimental conditions, an excellent fit between theoretical and experimental data was found, not only for collisions close to elasticity with low friction (collisions between pairs of billiard or steel balls), but also for collisions with relatively large friction and inelasticity (collisions between brass spheres). This finding supports the plausibility of the current formulation.

Furthermore, the current model enables us to justify quantitatively some practical rules for billiard games [5–7] Unusual postcollision paths can be predicted by varying the $R\omega_0/v_0$ and $R\Omega_0/v_0$ ratios by conveniently adjusting the impact point and orientation of the tapering rod. Figure 9 schematizes the predicted postcollision paths for the impact of a cue ball against a stationary ball for selected $R\omega_0/v_0$ values in the absence of initial pivoting angular velocity. Obviously, a more realistic account of inelasticity and frictional forces at impact would lead to a wide variety of postcollision paths. As an example, the rebound paths for a rolling sphere striking a vertical surface so that the frictional forces at impact are large enough to produce collision without sliding represented in Fig. 2 for selected $R\Omega_0/v_0 \cos\psi$ values.

To summarize, the model presented here makes possible a satisfactory description of sphere collisions in two dimmensions, allowing a direct estimate of the coefficients of restitution and friction, and provides an empirical criterion to discern between collisions with and without sliding.

1. J.H. Bayes and W.T. Scott, *Am. J. Phys.* **28** (1960) 197.
2. H.L. Armstrong, *Am. J. Phys.* **36** (1968) 56.
3. R.E. Wallace and M.C. Schroeder, *Am. J. Phys.* **56** (1988) 815.
4. G.Y. Onoda, *Am. J. Phys.* **57** (1989) 476.
5. V. Beltrán, *Rev. Mex. Fís.* **40** (1994) 323.
6. V. Beltrán, *Rev. Mex. Fís.* **42** (1996) 844.
7. J. Walker, *J. Sci. Am.* **249** (1983) 127.
8. F. Jiménez, *Rev. Esp. Fís.* **3** (1989) 31.
9. F. Jiménez, *Rev. Esp. Fís.* **3** (1989) 62.
10. A. Salazar and A. Sánchez-Lavega, *Eur. J. Phys.* **11** (1990) 228.
11. M. De la Torre, *Eur. J. Phys.* **15** (1990) 184.
12. R. Byrne, *Byrne's Treasury of Trick Shots in Pool and Billiards*, (Harcourt Brace Jovanovich Pub., 1982).
13. D.F. Griffing, *The Dynamics of Sports: Why That's the Way the Ball Bounces*, (Mohican Pub. Co., 1982).
14. A. Doménech and E. Casasús, *Phys. Educ.* **26** (1991) 186.
15. A. Doménech and M.T. Doménech, *Eur. J. Phys.* **9** (1988) 116.
16. A. Doménech and M.T. Doménech, *Eur. J. Phys.* **14** (1993) 177.
17. R.M. Brach, *J. Appl. Mech.* **51** (1984) 164.
18. T.R. Kane and D.A. Levinson, *Computat. Mech.* **2** (1985) 75.
19. J.B. Keller, *J. Appl. Mech.* **53** (1986) 1.
20. D.C. Hopkins and J.D. Patterson, *Am. J. Phys.* **45** (1977) 263.
21. G. Barnes, *Am. J. Phys.* **26** (1958) 5.
22. J.F. Bell, *Mechanics of Solids*, (Springer, Berlin, 1973).
23. H.L. Armstrong, *Am. J. Phys.* **53** (1985) 910.
24. J. Witters and D. Duymelinck, *Am. J. Phys.* **54** (1986) 80.